



Journal of Advanced Research in Fluid Mechanics and Thermal Sciences

Journal homepage:
https://semarakilmu.com.my/journals/index.php/fluid_mechanics_thermal_sciences/index
ISSN: 2289-7879



Characterization of a 3D Printed Self-Powered Micropump Mould for Microfluidics Application

Nur Ayreen Nafissa Mohd Asry¹, Nur Shamimi Amirah Md Sunhazim¹, Natrah Kamaruzaman¹, Ummikalsom Abidin^{1,*}

¹ School of Mechanical Engineering, Faculty of Engineering, Universiti Teknologi Malaysia, 81310 Johor Bahru, Johor, Malaysia

ARTICLE INFO

Article history:

Received 19 March 2022
Received in revised form 25 May 2022
Accepted 3 June 2022
Available online 30 June 2022

Keywords:

Self-powered micropump; microfluidics;
3D printed mould

ABSTRACT

The number of words should not exceed 350 Self-powered infusion micropump is a non-mechanical micropumps for microfluidics application. A three-dimensional (3D) printing is an intelligent additive manufacturing technique that permits cheap, fast and accurate geometrically complex designs. In this study, a self-powered infusion micropump master mould was fabricated using stereolithography (SLA) 3D printing technique and was characterized accordingly. Furthermore, polydimethylsiloxane (PDMS) self-powered micropump from the 3D printed mould was successfully replicated using soft lithography technique. Optical microscope with i-Solution Lite imaging software was used for micropump mould dimensions characterization. It was found that the smallest average percentage difference of 4.26 % was measured for straight inlet channel's width between the actual mould and the computer-aided design (CAD). The average coefficient of variance (CV) for all micropump components dimensions was 3.22. It was found that the SLA 3D printing reduced manufacturing time and costs by 30.43 % and 82.84 % respectively in comparison to the standard SU-8 mould. In conclusion, SLA 3D printing technology is a viable alternative to master mould fabrication in self-infusion micropump production since it accurately reproduced the design from the CAD input.

1. Introduction

Microfluidic systems have garnered significant interest over the last decade due to their ability to consolidate several laboratory operations onto a single chip, thereby permitting point-of-care testing (POCT) technology. Even though the size of the devices or operations is minimized, but the purpose of the systems is still maintained and can help to increase its functionality [1]. Glucose monitoring, hemostasis, cardiac indicators, drug screening, and pregnancy testing are all segments of the POC diagnostics market [2]. Although many sophisticated biochemical processes for POCT may be performed on-chip, a substantial portion of diagnostic procedures require the presence of active components such as pumps and valves to be practical. Additionally, the requirement of external bulky

* Corresponding author.

E-mail address: ummi@utm.my

<https://doi.org/10.37934/arfmts.97.1.127135>

power supply for active pumping is very unfeasible for point-of-care testing to be affordable and portable. Hence, the self-powered infusion micropump is a novel design solution for a passive pumping mechanism that flow is driven by capillary action.

Most of the microfluidic device fabrication has been accomplished by using soft-lithography with polydimethylsiloxane (PDMS) soft elastomers, which Duffy *et al.*, [3] group pioneered in 1998. However, this methodology necessitates the utilization of expensive and time-consuming cleanroom facilities for SU-8 molding, which is why alternative low-cost molding processes have recently gained prominence as reported by Faustino *et al.*, [4]. Furthermore, fabrication becomes more challenging with repetitive steps when a SU-8 mold is built to accommodate a range of microfluidic channel heights. Therefore, 3D printing has received substantial interest for master mold fabrication due to its exceptional ability to construct a complex three-dimensional object through a layer-by-layer manner in a short period of time [5].

The stereolithography (SLA) 3D printing process that employs resin photopolymerization with scanning UV light outperforms all other printing methods pertaining to high resolution and smooth surface. Recent advancements in SLA printing have increased vertical printing speed. Continuous liquid interface production (CLIP) is a novel SLA technology introduced by Tumbleston *et al.*, [6] that accelerates the process with an oxygen-permeable barrier preventing the polymerization at the solid interface in bat configuration, replacing the traditional layer-by-layer printing. In recent years, SLA applications in the medical field have been expanding, especially in orthognathic surgery [7].

SLA 3D printed part as a mold for soft lithography remains a challenge for curing inhibition of PDMS for all commercially available resins. Several authors [8-9] in their review suggested that pre-treatment with UV curing, surface cleaning and silanization prior to PDMS casting helps address this issue. The recent invention of custom-made resin has made it possible to cast PDMS directly against the printed mold without prior pre-treatment. Razavi Bazaz *et al.*, [10] successfully manufactured the micromixer and spiral microchip for liquid handling using this material.

This study critically evaluated the fabrication process of the master mold, focusing on its ease of fabrication, cost, timeliness, and features resolution from the comparison made on current technology. The adaptability of SLA technology in soft lithography was also established by demonstrating its ability to produce various microchannel geometries. The degree of accuracy of the SLA 3D printed mold was determined by percentage error evaluation on the dimensional characterization of the micropump.

2. Methodology

The 3D drawing of the micropump was designed using computer-aided design (CAD) software, SolidWorks. This functional model's design generally incorporates components to act as a particle separator such as vent holes, inlet and outlet holes, chambers for porous media and trapping magnetic particles, and channel tubes as shown in Figure 1. The micropump design has been revised from its initial version by Dal Dosso *et al.*, [11], with the width of the straight tube working liquid extended to 3 mm, which is sufficient to provide flow rate for liquid transport through the channel. Additionally, the micropump component is encased in a rectangular frame with 8 mm height to minimize PDMS spillage during the replication process. The CAD file of the design is exported to STL format for printing.

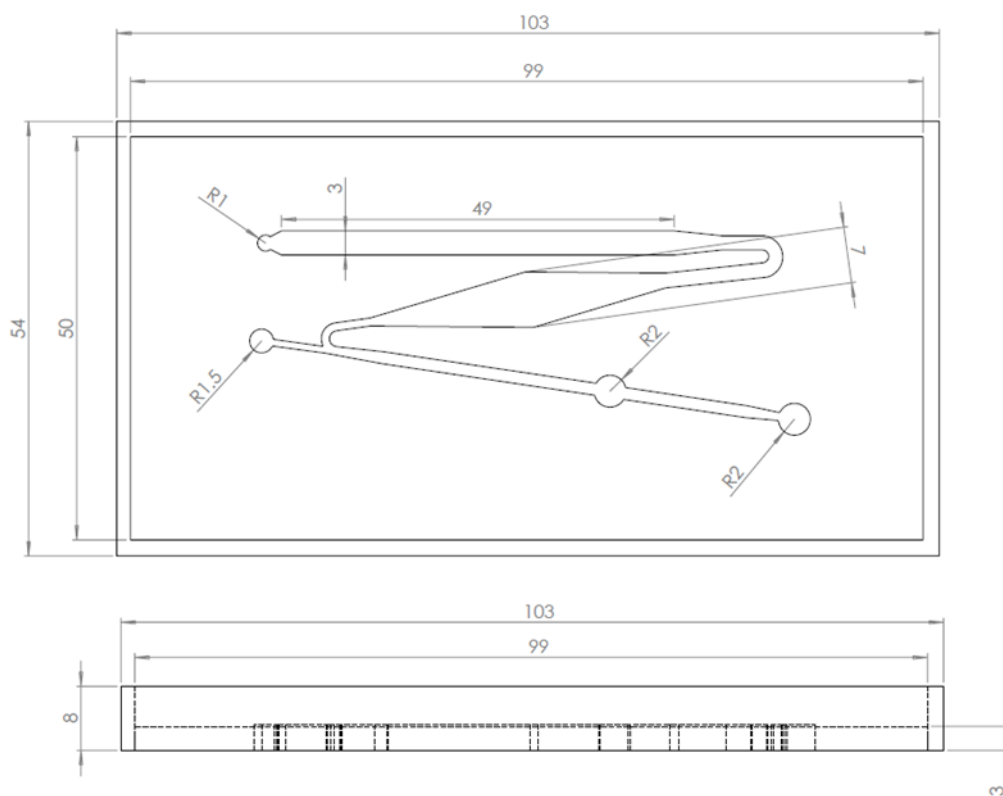


Fig. 1. Dimension of micropump design in mm

The master mold is printed in ABS-like resin using Zrapid SLA660 Industrial SLA 3D Printer (Zrapid Technologies Co., Ltd., Jiangsu, China). The printer can accommodate 600 x 600 x 300/350/400 printing volume of the mold with a Z-resolution of 100 μm . The finished G-code for the design model is uploaded over ethernet to the Zrapid controlling software, iSLA ZERO 5.0 for processing by the printer. During the printing process, a diode-pumped solid-state laser of UV light wavelength 355 nm is steered across the surface of vat photopolymer resin along the X-Y axis in accordance with the input CAD data. The resin solidifies due to photopolymerization, and the platform slides downward along the Z-axis for resin liquid application and subsequent curing. After printing was completed, the 3D printed mold was cleaned with ethanol, dried, and cured for 10 minutes under UV light.

The characterization was carried out under an optical microscope (RaxVision, USA) through Isolution Lite software connected with a computer monitor that displays real-time microscopic images of the 3D printed mold. The interest section of micropump components was captured at four different measurement points with a 0.65X magnification to study the printing quality.

3. Results

3.1 Comparison of Mold Fabrication

Essentially, the mold manufacturing in this study consists of two stages: microfluidic device designing in CAD software and mold production. Additional post-processing may be necessary depending on the surface finish of the mold, as is frequently inherent to the FDM printing mechanism. The soft-lithography with 3D printing technology simplifies manufacturing a microfluidic device from the conventional SU-8 molding, particularly by obviating the need for spin coating of SU-8 photoresist, soft baking, UV light exposure, post-exposure baking through a single printing process,

as shown in Table 1. The SU-8 method is more complicated in the final processing steps than SLA, which merely requires cleaning and post-curing.

Table 1

Mold fabrication process using photolithography SU-8 and 3D printing mechanisms

Description	SU8	FDM	SLA
CAD drawing	Required	Required	Required
Pre-processing	Wafer cleaning and heating	Filament installation and nozzle pre-heating	Resin pre-heating
Processing	SU-8 spin coating, soft baking, UV exposure, post-exposure baking	3D printing Extruding of ABS material on the heating bed layer by layer	3D printing UV light drawing of pre-programmed pattern on the surface of photopolymer layer by layer
Final processing	SU-8 development, rinse and dry, hard baking	Not required	Rinse and dry, post-curing
Post-processing	Not required	Sanding, polishing, smoothing with vapour acetone [11]	Not required

From the aforementioned mold fabrication process, there are several metrics for comparing 3D printed mould to the SU-8 mold, including overall duration of fabrication, cost per mold, and surface roughness of the mold as shown in Table 2.

From the design stage until the final step of prototype production, the duration to fabricate a microfluidic device was estimated. Based on past experiments, design optimization and PDMS replication could be completed within a few hours. However, SU-8 molding took the most prolonged duration for a complete fabrication according to the lead time specified by the manufacturing company. FDM 3D printing reduced the time by 60.87 % and SLA by 30.43 % from the overall fabrication time of SU-8 molding. In this case, FDM 3D printing is faster than SLA since the nozzle can extrude the molten material of a thicker layer with sparse infill. In contrast, SLA printing speed mainly depends on the fine laser beam scanning through the image on each layer which is much slower.

Next, SU-8 molding was the most expensive approach for fabricating a mold compared to 3D printing techniques. Numerous processes involved in SU-8 molding require numerous expensive materials, resulting in the highest overall production cost. With a single consumable material like filament or resin, 3D printing reduced the mold cost by 94.39 % and 82.84 % for FDM and SLA, respectively. The mold created from SLA 3D printing is more expensive due to the higher cost of resin than the filament spool that fed into the extruder of the FDM printer. SLA also requires replacing the building platform and the resin tank after a few litres of printing, which incurred a higher printing cost.

In terms of surface roughness, the SU-8 mould continues to be unrivalled in the fabrication of microfluidic devices due to its capacity to provide an extremely smooth surface finish with a value close to zero, as demonstrated in Table 2. It is discovered that the ABS-like mold created using the SLA printer had a smooth surface comparable to that of the SU-8 mould. In contrast, the mold created with an FDM printer such as ABS mold had a rough surface texture with visible layer line, resulting in higher average arithmetic mean deviation. Aside from encouraging the entrapment of air bubbles with the solid interface during PDMS replica molding, this rough surface finish will transfer the texture to PDMS. Moreover, the shear stress on the wall also increases, resulting in a pressure drop that affects the flow rate of the liquid moving through it.

Mold surface hydrophobicity is also an important factor in PDMS soft lithography to determine whether the surface modification is required to prevent PDMS from sticking to the mold. Based on

Table 2, the water contact angle (WCA) measurement revealed that all mould materials have generally hydrophobic surface qualities. On the surface of SU-8 and ABS molds, respectively, a silicon layer [13] and siliconizing agent [14] are typically used. While the ABS-like resin surface is proven hydrophobic by Son and Lee [15], the unreacted resin monomers on the printed mold may hinder the PDMS curing process, necessitating pre-treatment.

Table 2
Key parameters of different manufacturing mold strategies

Parameter	Unit	SU-8	FDM	SLA
Duration	days	23	9	16
Cost per mold	RM	1942	109	333
Surface Roughness	μm	0.04 [16]	9.42 [17]	1.43 [15]
Water contact angle	$^\circ$	90.0 [18]	95.0 [19]	79.4 [15]

3.2 SLA 3D PrinteMold

The ABS-like resin has comparable mechanical properties to ABS thermoplastic. There is no significant visible, apparent line on the surface feature for the printed part, as shown in Figure 2(a). As illustrated in Figure 2(b), this device accurately prints all micropump components' small structures according to the design input without any defects, even on parts prone to printing failure, such as the edge of a narrow microchannel and circumference of the holes. Figure 3 shows the peeled and cured PDMS replica mold that manage to be fabricated using the 3D printed mold.

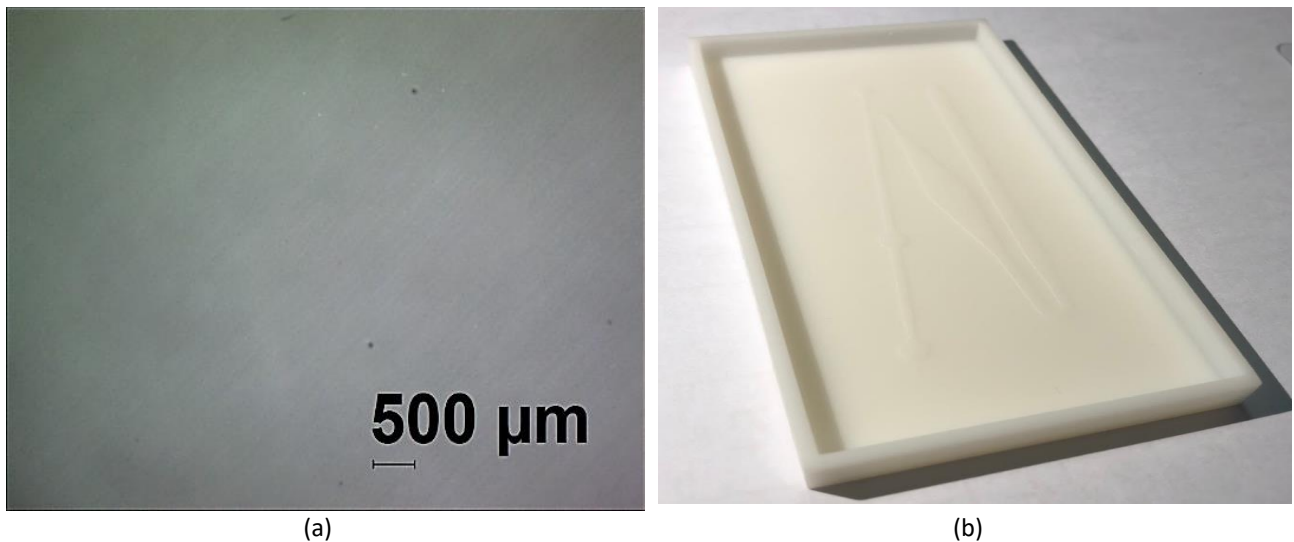


Fig. 2. 3D printed mold created by ZRapid SLA660 printer: (a) surface roughness with 1.5X magnification and (b) isometric view of micropump components



Fig. 3. Cured PDMS replica mold fabricated using 3D printed mold

3.2.1 Accuracy of SLA 3D Printing

The degree variation of the printed mold dimension from the specified design was analyzed in the form of error percentage for accuracy verification of SLA 3D printing. The sections of the micropump that were evaluated for this fabrication approach's feasibility are the inlet, outlet, and trapping chamber hole and the inlet and outlet channels.

As shown in Figure 4, the outlet hole has the highest percentage difference between its measured value and the actual design diameter, with a dimensional error of 94.79 %. The trapping chamber follows this with a deviation of 87.14 % and an inlet hole of 65.90 % percentage error. In contrast, the straight microchannels width of inlet and outlet have dimensional errors of 4.26 % and 8.95 %, respectively, which contributes an average of 6.61 % to the total percentage error. This variation demonstrated that the SLA printer creates better straight channels than circular cross-sectional areas for the microfluidic scale.

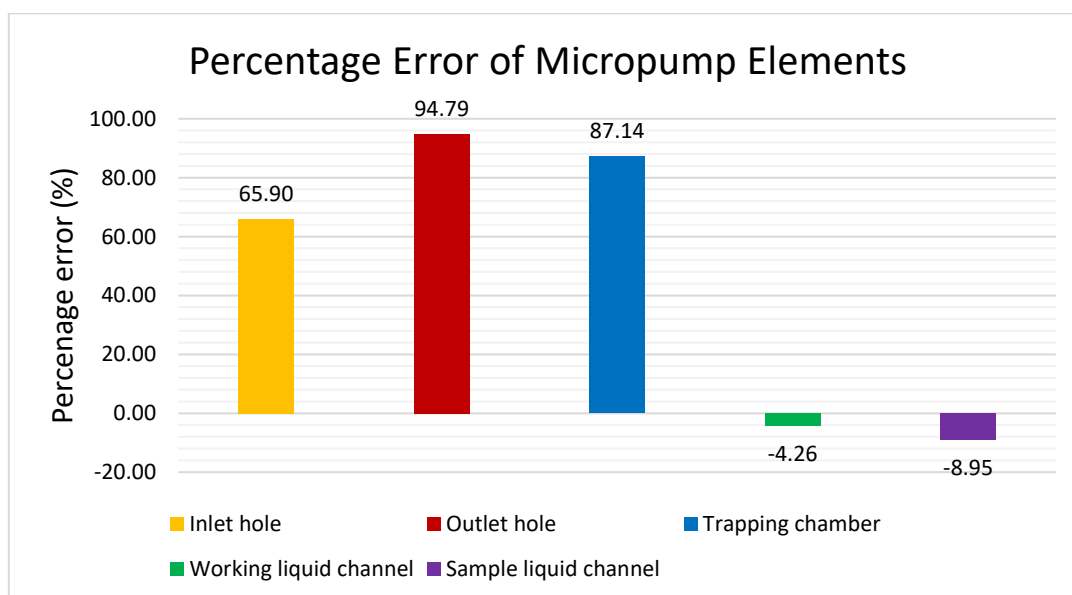


Fig. 4. Dimensional error of printed components from design value

In terms of coefficient of variation (CV) as shown in Figure 5, the inlet hole had the highest CV of 8.25. On the contrary, the CV of the trapping chamber hole is relatively low at 0.89. These values imply that the trapping chamber attained the highest level of measurement uniformity. It is worth noting that this printer can fabricate micropump components with a constant dimension from various points of measurement, which eventually yields a coefficient of variance 3.22, well below the accepted standard of 10.

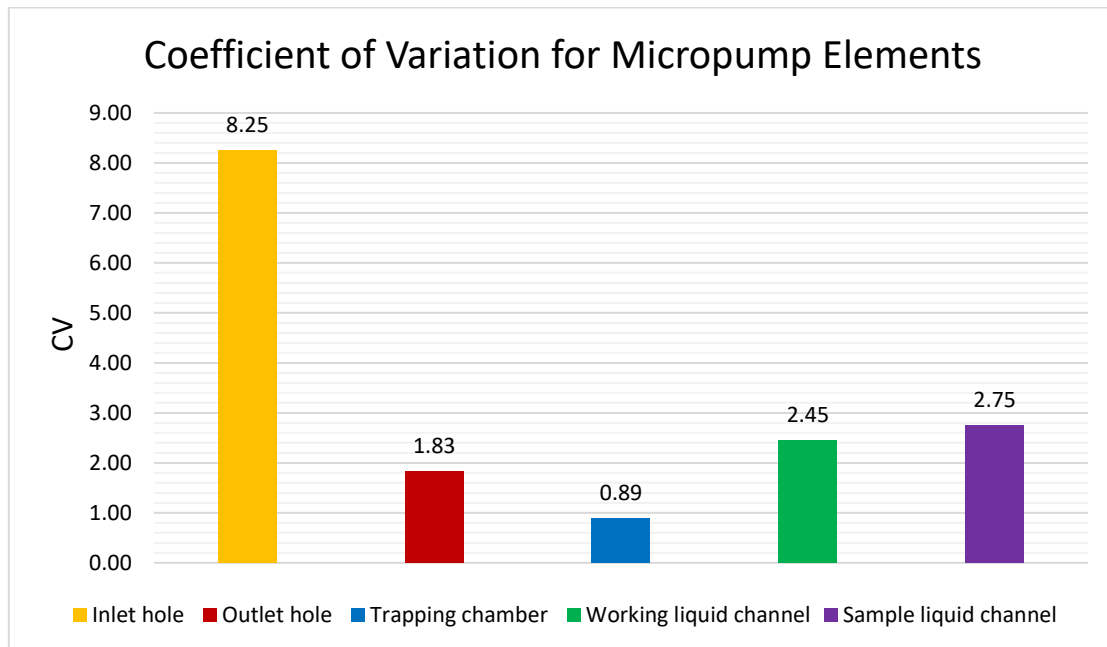


Fig. 5. Coefficient of variation of micropump design

Based on previous studies, the primary source of error in SLA 3D printing is associated with the printing setting and process, particularly with the light illuminated for resin curing in each layer. Al-Ahmari *et al.*, [20] reported that any scanner deflection shifts the propagating beam away from the target area, resulting in a significant error. One of the solutions recommended by Huang, Qin and Wang [21] to this problem is by employing projection-based stereolithography with a dynamic mask in a single exposure.

To establish the most appropriate printing mechanism for SIMPLE micropump fabrication, the geometrical error of an ABS-like mold was compared with the geometrical error of an ABS mold made using FDM 3D printing. The microchannel on both molds was seen to have shrunk in size with the negative percentage error as shown in Figure 6. The printed working liquid channel width of ABS mold deviates by 23.38 % from the planned value. Meanwhile, ABS-like mold has a minor dimensional error of 6.61 %. According to Alsoufi and Elsayed [22], the shrinkage of ABS material results in undesirable warping and distortion for FDM 3D printing. Similarly, volumetric shrinkage for the SLA process occurs during the resin photopolymerization, but the deformation is less pronounced than FDM.

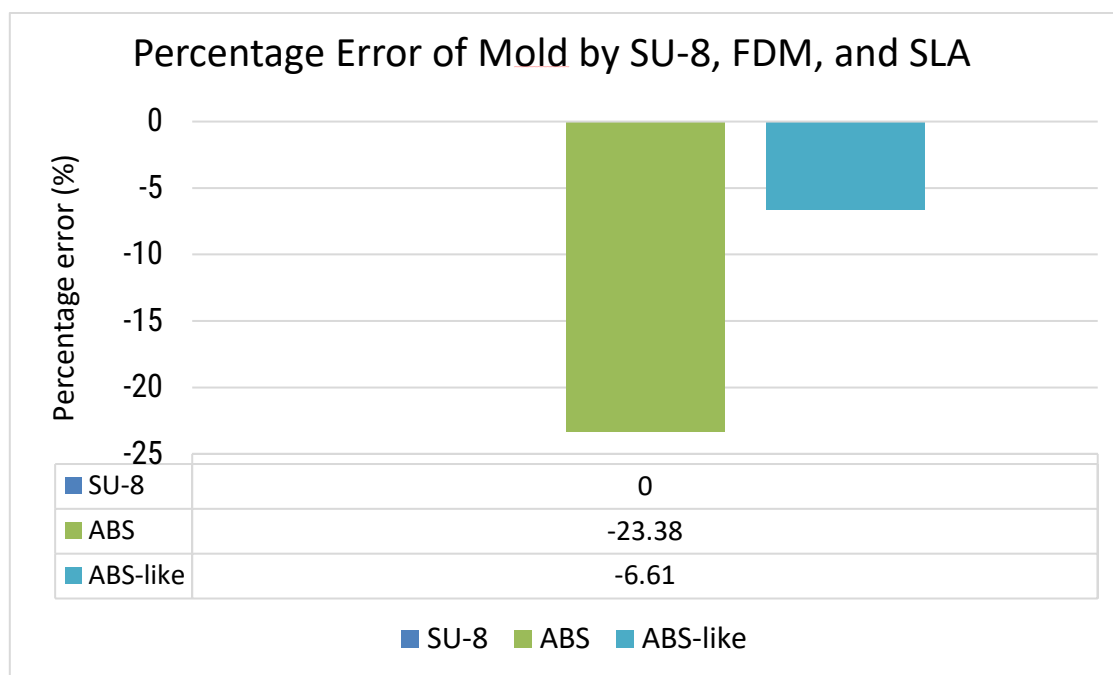


Fig. 6. Average dimensional error of SU-8, ABS and ABS-like molds

4. Conclusions

3D printing techniques are economical for prototyping and technologies enhance cost-effectiveness and speed; hence, it is advantageous for overcoming the complicated protocols associated with the use of SU-8. In comparison to SU-8 molding, the two distinct printing mechanisms, FDM and SLA, respectively, cut manufacturing time by 60.87 % and 30.43 % and cost by 94.39 % and 82.84 %. For fabrication quality assessment of SLA 3D printing, the circular cross-sectional area of the 3D printed mold exhibits high dimensional error, reaching up to 94.79 % for the diameter of the outlet hole. On the other hand, straight microchannels have dimensional errors at their inlet and outlet widths of 4.26 % and 8.95 %, respectively. The inlet hole has the highest CV of value 8.25, while the trapping chamber gives CV at a low value of 0.29. When comparing 3D printing of molds, it is observed that SLA generates features with a high degree of accuracy, as seen by the slight variation of microchannels from the actual structure, which averages 6.61 %, compared to 23.38 % for FDM. In conclusion, the SLA 3D printing technique successfully produced a master mold for the SIMPLE micropump.

Acknowledgement

This work was supported/funded by the Ministry of Higher Education under Fundamental Research Grant Scheme (FRGS/1/2019/TK03/UTM/02/2)

References

- [1] Mohamad Hafzan Mohamad Jowsey, Natrah Kamaruzaman and Mohsin Mohd Sies. "Heat and Flow Profile of Nanofluid Flow Inside Multilayer Microchannel Heat Sink." *Journal of Advanced Research in Micro and Nano Engineering* 4, no. 1 (2021): 1-9.
- [2] Park, Hyung Doo. "Current Status of Clinical Application of Point-of-Care Testing." *Archives of Pathology and Laboratory Medicine* 145, no. 2 (2021): 168–75. <https://doi.org/10.5858/arpa.2020-0112-RA>
- [3] Duffy, David C., J. Cooper McDonald, Olivier J.A. Schueller, and George M. Whitesides. "Rapid Prototyping of Microfluidic Systems in Poly(Dimethylsiloxane)." *Analytical Chemistry* 70, no. 23 (1998): 4974–84. <https://doi.org/10.1021/ac980656z>

- [4] Faustino, Vera, Susana O. Catarino, Rui Lima, and Graça Minas. "Biomedical Microfluidic Devices by Using Low-Cost Fabrication Techniques: A Review." *Journal of Biomechanics* 49, no. 11 (2016): 2280–92. <https://doi.org/10.1016/j.jbiomech.2015.11.031>
- [5] Kamei, Ken ichiro, Yasumasa Mashimo, Yoshie Koyama, Christopher Fockenber, Miyuki Nakashima, Minako Nakajima, Junjun Li, and Yong Chen. "3D Printing of Soft Lithography Mold for Rapid Production of Polydimethylsiloxane-Based Microfluidic Devices for Cell Stimulation with Concentration Gradients." *Biomedical Microdevices* 17, no. 2 (2015). <https://doi.org/10.1007/s10544-015-9928-y>
- [6] Tumbleston, John R, David Shirvanyants, Nikita Ermoshkin, Rima Januszewicz, Ashley R Johnson, David Kelly, Kai Chen, et al. "Continuous Liquid Interface of 3D Objects." *Science* 347, no. 6228 (2015): 1349–52. <https://doi.org/10.1126/science.aaa2397>
- [7] Shujaat, Sohaib, Oliver da Costa Senior, Eman Shaheen, Constantinus Politis, and Reinhilde Jacobs. "Visual and Haptic Perceptibility of 3D Printed Skeletal Models in Orthognathic Surgery." *Journal of Dentistry* 109, no. 1 (2021): 103660. <https://doi.org/10.1016/j.jdent.2021.103660>
- [8] Shrestha, Jesus, Maliheh Ghadiri, Melane Shanmugavel, Sajad Razavi Bazaz, Steven Vasilescu, Lin Ding, and Majid Ebrahimi Warkiani. "A Rapidly Prototyped Lung-on-a-Chip Model Using 3D-Printed Molds." *Organs-on-a-Chip* 1, no. 1 (2019): 100001. <https://doi.org/10.1016/j.ooc.2020.100001>
- [9] Waheed, Sidra, Joan M. Cabot, Niall P. Macdonald, Umme Kalsoom, Syamak Farajikhah, Peter C. Innis, Pavel N. Nesterenko, Trevor W. Lewis, Michael C. Breadmore, and Brett Paull. "Enhanced Physicochemical Properties of Polydimethylsiloxane Based Microfluidic Devices and Thin Films by Incorporating Synthetic Micro-Diamond." *Scientific Reports* 7, no. 1 (2017): 1–10. <https://doi.org/10.1038/s41598-017-15408-3>
- [10] Razavi Bazaz, Sajad, Navid Kashaninejad, Shohreh Azadi, Kamal Patel, Mohsen Asadnia, Dayong Jin, and Majid Ebrahimi Warkiani. "Rapid Softlithography Using 3D-Printed Molds." *Advanced Materials Technologies* 4, no. 10 (2019): 1–11. <https://doi.org/10.1002/admt.201900425>
- [11] Dal Dosso, Francesco, Yura Bondarenko, Tadej Kokalj, and Jeroen Lammertyn. "SIMPLE analytical model for smart microfluidic chip design." *Sensors and Actuators A: Physical* 287 (2019): 131-137. <https://doi.org/10.1016/j.sna.2019.01.005>
- [12] Wickramasinghe, Sachini, Truong Do, and Phuong Tran. "FDM-Based 3D Printing of Polymer and Associated Composite: A Review on Mechanical Properties, Defects and Treatments." *Polymers* 12, no. 7 (2020): 1–42. <https://doi.org/10.3390/polym12071529>
- [13] Olanrewaju, A. O., A. Robillard, M. Dagher, and D. Juncker. "Autonomous Microfluidic Capillaric Circuits Replicated from 3D-Printed Molds." *Lab on a Chip* 16, no. 19 (2016): 3804–14. <https://doi.org/10.1039/C6LC00764C>
- [14] Baker, Christopher A., Leonard K. Bright, and Craig A. Aspinwall. "Photolithographic Fabrication of Microapertures with Well-Defined, Three-Dimensional Geometries for Suspended Lipid Membrane Studies." *Analytical Chemistry* 85, no. 19 (2013): 9078–86. <https://doi.org/10.1021/ac401639n>
- [15] Son, Jungyu, and Hyunseop Lee. "Preliminary Study on Polishing SLA 3D-Printed ABS-like Resins for Surface Roughness and Glossiness Reduction." *Micromachines* 11, no. 9 (2020). <https://doi.org/10.3390/mi11090843>
- [16] Ayoib, A., U. Hashim, M. K.M. Arshad, and V. Thivina. "Soft Lithography of Microfluidics Channels Using SU-8 Mould on Glass Substrate for Low Cost Fabrication." *IECBES 2016 - IEEE-EMBS Conference on Biomedical Engineering and Sciences*, 2016, 226–29. <https://doi.org/10.1109/IECBES.2016.7843447>
- [17] Jayanth, N., P. Senthil, and C. Prakash. "Effect of Chemical Treatment on Tensile Strength and Surface Roughness of 3D-Printed ABS Using the FDM Process." *Virtual and Physical Prototyping* 13, no. 3 (2018): 155–63. <https://doi.org/10.1080/17452759.2018.1449565>
- [18] Kumar, Vijay, and Niti Nipun Sharma. "Synthesis of Hydrophilic to Superhydrophobic SU8 Surfaces." *Journal of Applied Polymer Science* 132, no. 18 (2015): 1–10. <https://doi.org/10.1002/app.41934>
- [19] Abourayana, Hisham, Peter Dobbyn, and Denis Dowling. "Enhancing the Mechanical Performance of Additive Manufactured Polymer Components Using Atmospheric Plasma Pre-Treatments." *Plasma Processes and Polymers* 15, no. 3 (2018). <https://doi.org/10.1002/ppap.201700141>
- [20] Al-Ahmari, Abdulrahman, Mohammed Ashfaq, Syed Hammad Mian, and Wadea Ameen. "Evaluation of Additive Manufacturing Technologies for Dimensional and Geometric Accuracy." *International Journal of Materials and Product Technology* 58, no. 2–3 (2019): 129–54. <https://doi.org/10.1504/IJMPT.2019.097665>
- [21] Huang, Jigang, Qin Qin, and Jie Wang. "A Review of Stereolithography: Processes and Systems." *Processes* 8, no. 9 (2020). <https://doi.org/10.3390/pr8091138>
- [22] Alsoufi, Mohammad S., and Abdulrhman E. Elsayed. "Surface Roughness Quality and Dimensional Accuracy—A Comprehensive Analysis of 100% Infill Printed Parts Fabricated by a Personal/Desktop Cost-Effective FDM 3D Printer." *Materials Sciences and Applications* 09, no. 01 (2018): 11–40. <https://doi.org/10.4236/msa.2018.91002>